04

The study of the process of hydrogenation of single-walled carbon nanotubes using inductively coupled argon-hydrogen plasma

© E.I. Preobrazhensky,[1] A.V. Vodopyanov,[1,2] A.V. Nezhdanov[2]

[1] Institute of Applied Physics, Russian Academy of Sciences,
603950 Nizhny Novgorod, Russia
[2] Lobachevsky University of Nizhny Novgorod,
603022 Nizhny Novgorod, Russia
e-mail: evgenypr@ipfran.ru

Received April 5, 2023
Revised April 5, 2023
Accepted April 5, 2023

In this article it was demonstrated the possibility of partial hydrogenation of single-walled carbon nanotubes using an inductively coupled argon-hydrogen plasma. It was studied the changes in the Raman spectrum of samples of single-walled carbon nanotubes during plasma hydrogen intercalation with depending on the treatment time, the discharge power, the substrate material on which the nanotubes were deposited, and the control external voltage. The predominant role of hydrogen ions in the hydrogenation of single-walled carbon nanotubes has been demonstrated.

Keywords: plasma chemistry, single-walled carbon nanotubes, hydrogenation,inductively coupled plasma, SWCNTs.

DOI: 10.61011/TP.2023.07.56622.71-23

Introduction

Great attention is paid in the present-day world to research into new materials; specifically, a great number of studies concerned with two-dimensional materials are being published. A considerable fraction of these deal with two-dimensional carbon structures [1]. Owing to its unique properties, graphene [2] was in the focus of attention. Graphene and carbon nanomaterials of a similar structure are fine electricity and heat conductors and feature a very large specific surface area and a high strength factor [3], which make them applicable in the design of various devices (e.g., biosensors) [4]. The possibility of intercalation with various atoms, such as hydrogen [5], is another potentially applicable feature of graphene that is also worthy of note. Hydrogenated graphene (graphane) may be produced in a number of ways (e.g., by thermal decomposition or chemically [6]). This two-dimensional hydrogen modification of graphene may be applied as a material for hydrogen storage [7] or in the fabrication of biosensors [4]. In contrast to graphene with zero band gap, graphane or partially hydrogenated graphene are semiconductors with potential for band-gap engineering performed by varying the amount of hydrogen incorporated into the lattice [8]. Thus, gradual hydrogenation of graphene allows one to produce materials with the desired „intermediate“ (between graphene and graphane) thermal and conducting properties [9]. Another important feature of hydrogenated graphene is its capacity to release hydrogen under the influence of temperature [10].

The techniques for production of graphene have improved greatly since the days of its discovery. However, the process of fabrication of graphene (especially freely suspended one) still remains fairly costly, complicated, and unsuitable for mass production [11]. That said, carbon nanotubes may be regarded in a first approximation as folded graphene. Their properties are close to those of graphene; specifically, they may also be functionalized with hydrogen (hydrogenated) [12–14]. Nanotubes also have an advantage in being relatively inexpensive to produce and, consequently, freely available. Note that carbon nanotubes may be regarded as „defective“ graphene. On the one hand, their degree of hydrogenation may be much lower than the one of graphene, since they have a folded tubular structure; on the other hand, defects in the form of a side wall facilitate the formation of carbon–hydrogen bonds in the lattice [13]. The aim of the present study is to examine the process of hydrogenation of carbon nanotubes in low-pressure argon–hydrogen plasma at various parameter values.

1. Experimental setup and diagnostic techniques

A series of experiments into hydrogenation of carbon nanotubes deposited onto different substrates was performed. Single-walled carbon nanotubes TUBALL, which were used in our experiments, were produced by CVD. In what follows, the term „nanotubes“ denotes single-walled carbon nanotubes (SWCNTs). A plasma discharge was initiated in a quartz tube 4 cm in diameter with an inductor wound round it. An Advanced Energy Cesar generator operated at 13.56 MHz was used as a radio-frequency electromagnetic field source. The maximum power was 600 W. A plasma discharge was initiated in a mixture of argon and hydrogen

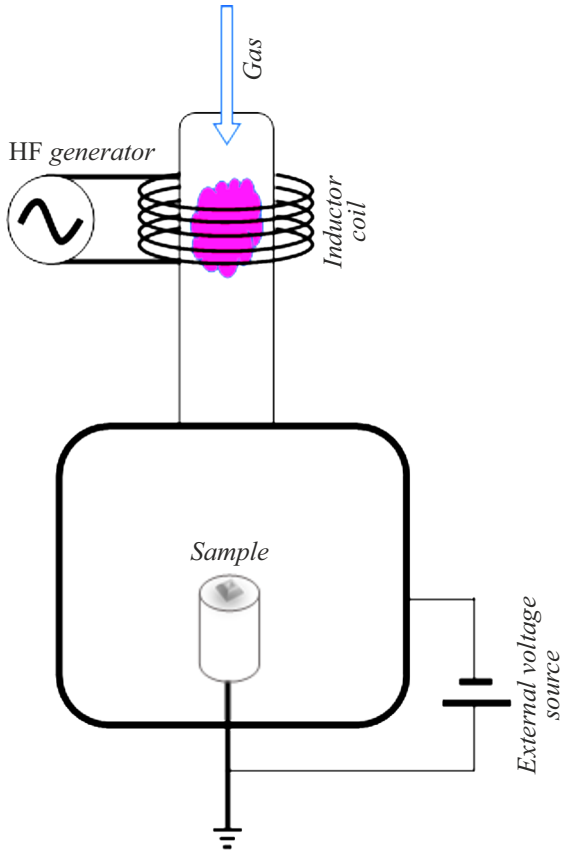

Figure 1. Diagram of the experimental setup.

under a pressure of 60 mTorr. The power supplied to the discharge was 50–200 W. The chamber was evacuated in advance to a pressure of 10^{-5} mTorr in order to exclude the possibility of contamination by impurities from air. Gas was supplied via a Bronkhorst lowdP series flow regulator. The argon and hydrogen flow was maintained at 127 and 26 sccm, respectively. The key advantage of this setup consists in the fact that a radio-frequency inductively coupled plasma discharge is electrodeless and allows one to produce pure plasma (i.e., plasma with no impurities due to electrode erosion). The design of the plasma setup is similar to the one used in our previous study [9]. To „accelerate“ hydrogenation further, a constant external voltage was applied between the chamber and a table on which the samples were positioned. An additional potential difference should raise the number of ions in the vicinity of a sample, thus altering the graphene hydrogenation rate. If no external voltage was applied, the table was grounded. The schematic diagram of the setup is shown in Fig. 1.

Nanotube samples deposited onto a substrate were positioned within 30 cm from the discharge center on the grounded brass table. The concentration and temperature of electrons at the sample position were measured with a double probe. At a distance of 30 cm from the inductor center, $T_e \approx 6$ eV and $N_e \approx 5 \cdot 10^7$ cm^{-3} at a plasma discharge power of 50 W. According to the results of preliminary experiments, the electron concentration increases with increasing power or decreasing distance between the discharge center and the probe (roughly following an inverse square law), while the electron temperature varies only slightly. To secure nanotubes on a glass or stainless-steel substrate, they were mixed with 96% ethanol, deposited onto a degreased surface and dried for 1 h until ethanol was removed completely from a sample.

Raman spectroscopy was used as the primary technique for determination of the degree of SWCNT hydrogenation. This method is sufficiently sensitive to detect bonds forming in the lattice of carbon nanostructures after plasma processing. In addition, the method is nondestructive. Spectra of samples were measured using an NTEGRA Spectra system (NT-MDT, Zelenograd, Russia) at room temperature within the $50-3300\,\text{cm}^{-1}$ range with a resolution of $2\,\text{cm}^{-1}$. The laser wavelength was 473 nm. The error of spectrum recording was 5%. It was found that carbon nanostructures had two characteristic peaks in Raman spectra: G ($1580\,\text{cm}^{-1}$) and $2D$ ($2680\,\text{cm}^{-1}$) [3,15]. The $2D$ peak characterizes the monolayer nature of samples with no defects [5]. The G peak indicates that the sample structure corresponds to a regular hexagonal structure with a side of 1.42 Å [3] and sp^2 hybridization. As the amount of hydrogen in the structure increases, additional peaks emerge: D at $1350\,\text{cm}^{-1}$ and $D+D'$ at $2950\,\text{cm}^{-1}$ [3]. The D peak is induced by sp^3 hybridization or defects [3]. Examples of such defects are layering and twisting of the structure (intrinsic to carbon nanotubes) or a slight initial mismatch with an ideal hexagonal lattice. The presence of peak $D+D'$ is indicative of attachment of hydrogen to graphene [16]; presumably, it is also true in the case of carbon nanotubes. This is related to the fact that a Raman spectrum may have features at 2857 and $2915\,\text{cm}^{-1}$ induced by symmetric and asymmetric modes of valence C–H vibrations [16]. Just as in our previous study for graphene [9], we follow the hypothesis from [5] and assume that hydrogen is uniquely responsible for the formation of defects in carbon nanotubes. This point is arguable for the following reasons. First, the used experimental parameters allow one to produce relatively low-power plasma, which does not induce sample degradation in the course of experiments. The second reason is the fact that argon is an inert gas and interacts only weakly with samples. It is used to suppress the influence of hydrogen plasma on samples. In addition, it was taken into account that carbon nanotubes are durable, and bombardment with inert argon atoms is thus likely to have an insignificant effect on structural defects at a relatively short exposure time and a sufficiently low electron temperature. The ratio of intensities of peaks $I(D)$ and $I(G)$ serves as a hydrogenation indicator in the present study. Attention is also paid to an additional hydrogenation measure: the ratio of intensities of peaks $I(D+D')/I(D)$, since peak $D+D'$ indicates the presence of carbon–hydrogen bonds [16]. Raman spectra were normalized to peak G in processing.

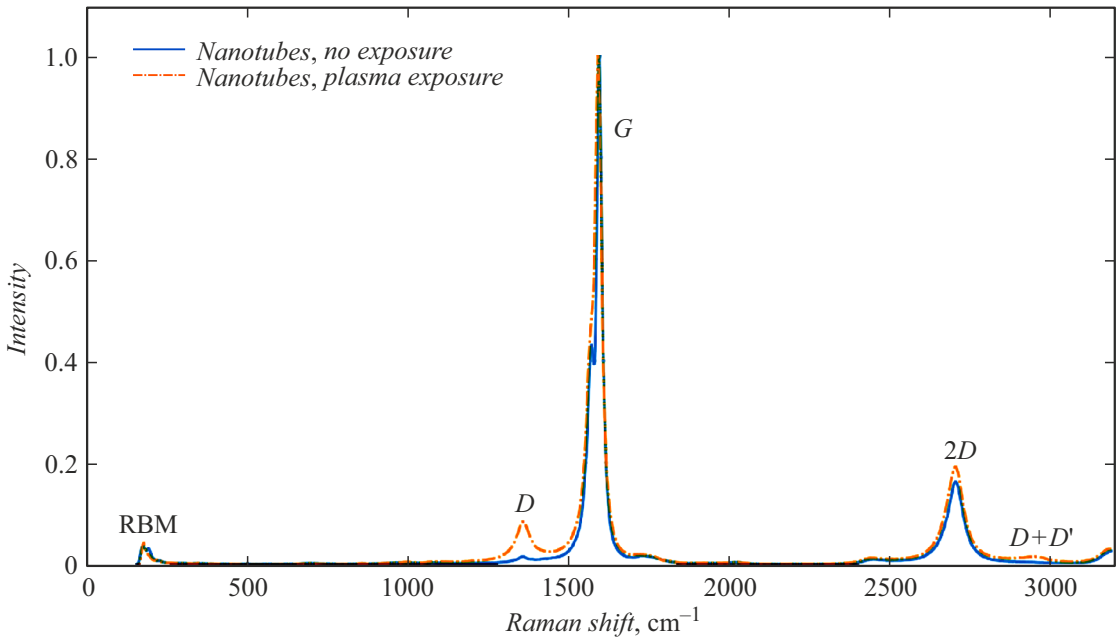

Figure 2. Normalized Raman spectra of SWCNTs before and after exposure to plasma.

2. Experimental results

The general characteristic spectrum of samples in shown in Fig. 2. Peak $2D$, which is typical of single-walled carbon nanotubes, and split peak G are present in the Raman spectra of samples [17]. Characteristic weak peaks D and $D + D'$ manifest themselves in the spectra of samples processed in plasma. In what follows, normalized plots are cut off at an intensity level of 0.21 to demonstrate peaks D and $D + D'$. Characteristic weak peaks G' at 2450 [16] and a peak at $1750\,\mathrm{cm}^{-1}$ are also seen in the spectrum. It is assumed that they are related to the very structure of single-walled carbon nanotubes, since they do not vanish after exposure to plasma. Similar peaks were reported in [18] and [19]. They may be associated with single-phonon or two-phonon second-order double resonance processes [20]. The characteristic positioning of the radial breathing mode (RBM) at $180\,\mathrm{cm}^{-1}$ and the lack of additional peaks at $> 200\,\mathrm{cm}^{-1}$ [21] suggest that samples are single-walled carbon nanotubes.

2.1. Influence of the substrate material on nanotube hydrogenation

Samples on dielectric (glass) and metal (stainless steel) substrates were prepared in order to examine the influence of the substrate material on SWCNT hydrogenation in plasma. The same discharge parameters were set in plasma processing of nanotube samples on different substrates. The exposure time was 10 min, and the discharge power was 50 W. The pressure was maintained at 60 mTorr. The results of processing of Raman spectra recorded in this series of experiments are presented in Fig. 3. Ratios of intensities of peaks $I(D)/I(G)$ and $I(D + D')/I(G)$ for Raman spectra of samples on different substrates are listed in the table.

It can be seen from Fig. 3 and the table that the degree of hydrogenation (i.e., parameter $I(D)/I(G)$) increases after plasma processing of nanotubes on metal substrates. The spectra for samples on glass remained almost unchanged. The emergence of peak $D + D'(3000\,\mathrm{cm}^{-1})$ was also noted on metal substrates. This is indicative of successful partial hydrogenation of nanotubes on a copper substrate. A significant reduction in the hydrogenation rate on glass substrates may be explained in the following way. It is fair to assume that charges accumulate in a sample on a glass substrate. Within a fairly short (compared to the exposure time) interval of time, the charge at carbon nanotubes accumulated in the course of interaction with active hydrogen from a plasma discharge becomes so significant that ions get repelled. According to estimates, a sample may be charged to a potential of 30 V within 1 μs at typical parameters of the experiment. In addition, the results of experiments indicate that the process of intercalation of nanotubes on glass is very slow and requires a greater power supplied to plasma. In the case of a metal substrate, the charge leaks freely from carbon nanotubes, and an ion-repelling electric field is not generated. It follows from the above that intercalation is likely to be driven primarily by hydrogen ions. Atoms and molecules of hydrogen produce a smaller contribution to graphene hydrogenation.

2.2. Influence of the exposure time on SWCNT hydrogenation

A series of experiments aimed at examining the influence of the exposure time on SWCNT hydrogenation on a metal

Ratios of intensities of peaks $I(D)/I(G)$ and $I(D+D')/I(G)$ for SWCNTs deposited onto different substrates before and after plasma processing

Ratio of intensities of peaks	Glass substrate, no exposure	Glass substrate, 50 W, 10 min	Metal substrate, no exposure	Metal substrate, 50 W, 10 min
$I(D)/I(G)$	0.0168 ± 0.0025	0.0108 ± 0.004	0.0153 ± 0.0019	0.0507 ± 0.004
$I(D+D')/I(G)$	0.0042 ± 0.0006	0.003 ± 0.001	0.0039 ± 0.0004	0.0094 ± 0.0007

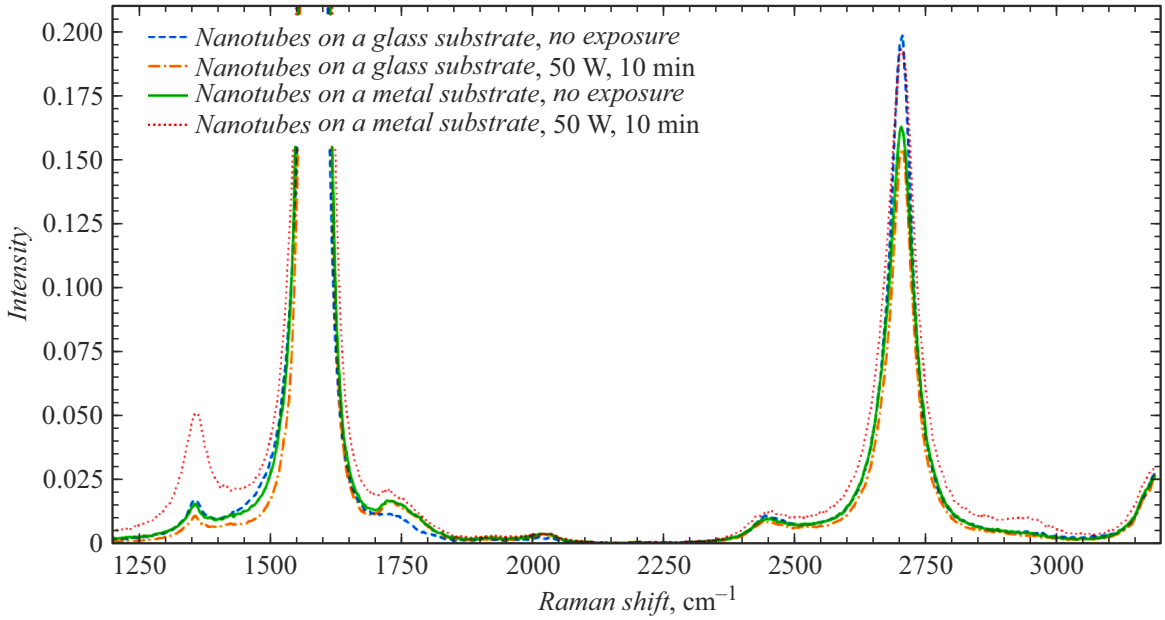

Figure 3. Normalized Raman spectra of SWCNTs deposited onto different substrates before and after plasma processing (10 min, 50 W, 60 mTorr). Blue dashed and green solid curves (in the online version) represent the spectra of carbon nanotubes on glass ans metal substrates, respectively, measured prior to processing. Orange dash-and-dot and red dotted curves (in the online version) represent the spectra of carbon nanotubes on glass ans metal substrates, respectively, measured after processing.

substrate was performed next. Figure 4, *a* shows normalized Raman spectra of the as-prepared sample and samples on a metal substrate exposed for 2, 10, and 30 min. The sample table was grounded. Figures 4, *b, c* present the ratios of intensities of peaks $I(D)/I(G)$ and $I(D+D')/I(G)$, respectively, corresponding to different exposure times. The exposure parameters were as follows: a pressure of 60 mTorr and a discharge power of 50 W.

It is evident that the degree of hydrogenation increases with exposure time. It should also be noted that the rate of hydrogenation decreases. This is attributable to the fact that the number of „free“ carbon atoms in the lattice, which may potentially form a bond with hydrogen, decreases with time. It is fair to assume that samples undergo degradation at longer exposures; as was observed in experiments with graphene [10], long-term processing in plasma has a destructive influence on samples. It follows from Fig. 4, *c* that the intensity of the peak associated with C−H bonding starts decreasing at a certain point in time; this provides additional evidence of the destructive effect of long-term processing under the given discharge conditions.

2.3. Influence of the discharge power on SWCNT hydrogenation

Figure 5, *a* shows the variation of normalized Raman spectra of SWCNT samples on a metal substrate, which were positioned on the grounded brass table, with power supplied to plasma. The exposure time was 30 min. The pressure in the chamber was maintained at 60 mTorr. Figures 5, *b, c* present the ratios of intensities of peaks $I(D)/I(G)$ and $I(D+D')/I(G)$, respectively, corresponding to different discharge powers.

One can see that the degree of hydrogenation increases with increasing plasma discharge power. This is manifested in the general trend of variation of both $I(D)/I(G)$ and $I(D+D')/I(G)$ intensity ratios. It may also be noted that the rate of growth of these ratios decreases at power increases further.

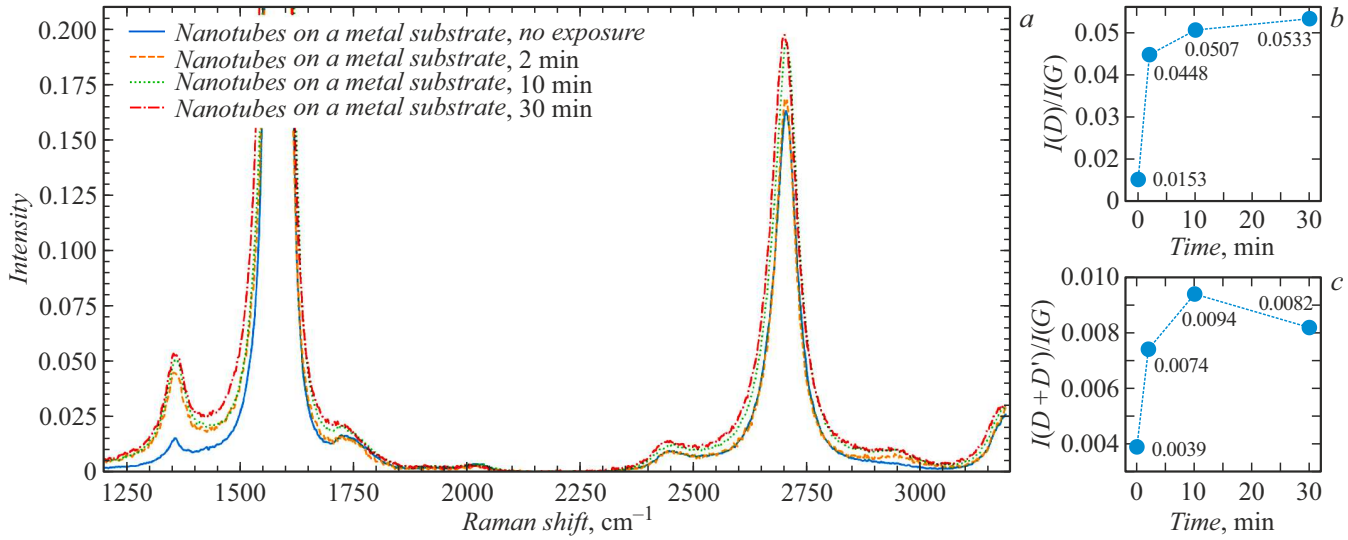

Figure 4. Normalized Raman spectra of SWCNTs (a) corresponding to different exposure times. Solid blue curve (in the online version) — as-prepared sample, dashed orange curve (in the online version) — 2 min of exposure to plasma, dotted green curve (in the online version) — 10 min, and dash-and-dot red curve (in the online version) — 30 min. b and c — Ratios of intensities of peaks $I(D)/I(G)$ and $I(D+D')/I(G)$, respectively, for SWCNTs at different exposure times. Plasma discharge parameters: 60 mTorr and 50 W.

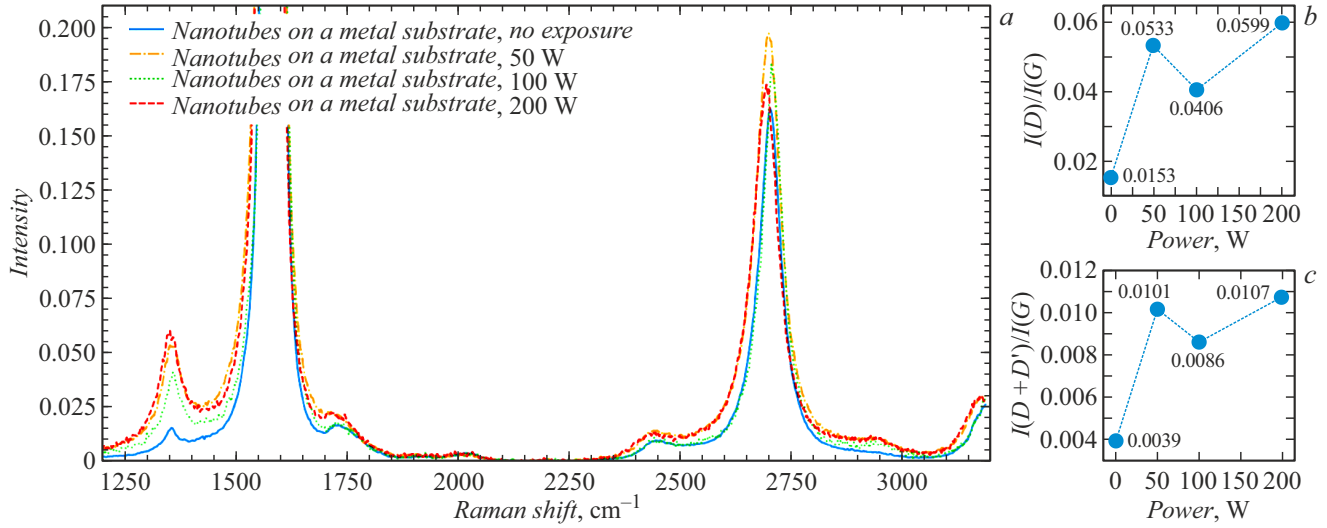

Figure 5. Normalized Raman spectra of SWCNTs (a) corresponding to different discharge powers. Solid blue curve (in the online version) — as-prepared sample, dash-and-dot orange curve (in the online version) — 50 W, dotted green curve (in the online version) — 100 W, and dashed red curve (in the online version) — 200 W. Ratios of intensities of peaks $I(D)/I(G)$ (b) and $I(D+D')/I(G)$ (c) for SWCNTs at different discharge powers. Parameters of the experiment: 60 mTorr and 30 min of exposure to plasma.

Experiments with increasing levels of power supplied to plasma were also carried out for samples on glass. At an exposure time of 30 min and different power levels, both peak D did not grow appreciably in amplitude relative to G and peak $D+D'$ did not emerge. In addition, experiments with the exposure time varying from 2 to 30 min were performed for samples on a glass substrate at a power of 50 W. Hydrogenation ceased almost completely. This provides additional evidence in favor of the notion that the degree of hydrogenation of nanotubes on glass is very low and that SWCNTs react primarily with hydrogen ions.

2.4. Variation of nanotube hydrogenation with voltage applied to the table

The effect of an external constant voltage on SWCNT hydrogenation was examined in a series of experiments. The voltage was applied between the chamber and the table on which carbon nanotubes were positioned. Figures 6, *a, d* show the variation of Raman spectra of samples on metal and dielectric substrates, respectively, with voltage applied to the table. The „+“ and „−“ signs correspond to the sign of the applied external voltage. Figures. 6, *b, c*

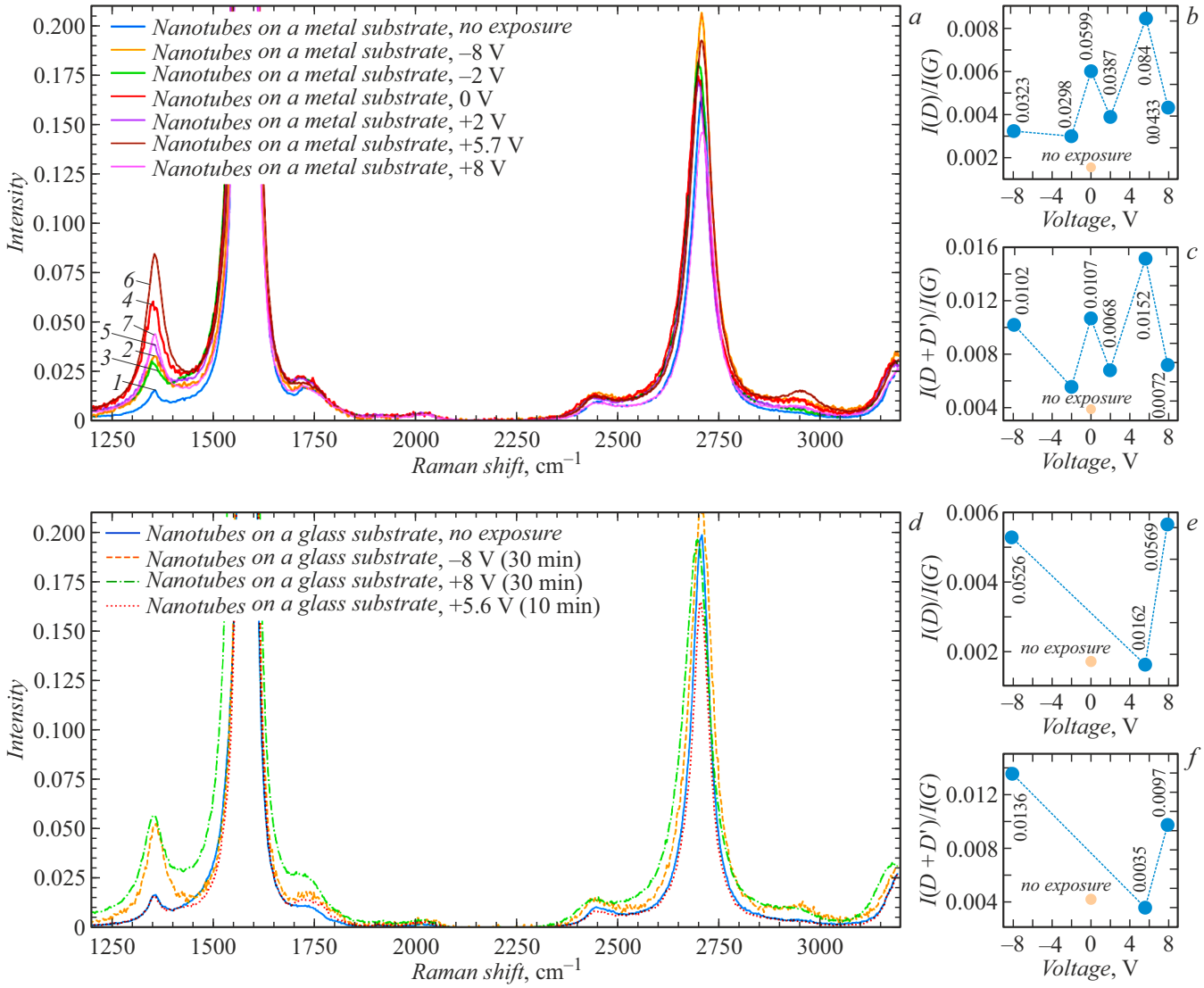

Figure 6. Normalized Raman spectra of SWCNT samples on a metal (a) substrate at -8 (*2*), -2 (*3*), 0 (*4*), $+2$ (*5*), $+5.7$ (*6*), and $+8$ V (*7*) between the table and the chamber; *1* —as-prepared samples. Spectra of SWCNT samples on a dielectric (*d*) substrate with an applied external voltage of -8 V (30 min of exposure to plasma, dashed orange curve (in the online version)), $+8$ V (30 min, dash-and-dot green curve (in the online version)), $+5.6$ V (10 min, dotted red curve (in the online version)); the as-prepared sample is represented by the solid blue curve (in the online version)). Ratios of intensities of peaks $I(D)/I(G)$ and $I(D+D')/I(G)$ for metal (*b* and *c*, respectively) and dielectric (*e* and *f*, respectively) substrates. The exposure time is 30 min, the discharge power is 200 W, and the pressure is 60 mTorr. The spectrum of SWCNTs on glass corresponding to the same plasma parameters, zero external voltage, and an exposure time of 10 min is shown in $d-f$ for comparison.

present the ratios of intensities of peaks $I(D)/I(G)$ and $I(D+D')/I(G)$ for samples on a metal substrate, while Figs.. 6, *e,f* present similar data for a dielectric substrate. In the case of samples on a metal substrate, the voltage is effectively applied to nanotubes. The exposure time was 30 min in each experiment, the discharge power was 200 W, and the pressure in the chamber was 60 mTorr. The spectra of SWCNTs on glass corresponding to the same discharge parameters, zero external voltage, and an exposure time of 10 min are shown in Figs. 6, $d-f$ for comparison. The voltage values of $+5.7$ V in Fig. 6, *a* and $+5.6$ V in Fig. 6, *d* were measured with the table insulated.

The spectra in Figs. 6, *a, d* suggest that an external constant voltage has a fairly significant effect on hydrogenation. It may be concluded that, in addition to being quite resistant to hydrogenation, SWCNTs on a glass substrate are hydrogenated primarily by hydrogen ions at the indicated discharge parameters. It is rather hard to determine a functional dependence of the ratio of intensities of peaks on voltage. A subtle general trend of an increase in the efficiency or rate of hydrogenation at higher positive voltages applied to the table may be noted. A more pronounced trend of an increase in the degree of hydrogenation upon the application of a positive voltage to the table suggests that

negative hydrogen ions react more actively with graphene than positive ones.

Conclusion

The results of experiments on SWCNT hydrogenation allow one to conclude that hydrogen intercalation is, in general, fairly efficient (proceeds at a considerably high rate). It is evident that, if an external voltage is not applied, nanotubes positioned on a conducting material are hydrogenated much more efficiently. At the same time, it turned out that the substrate material has almost no effect on hydrogenation if an external bias voltage is applied to the table. It was demonstrated that the bias voltage has a significant influence on the end result if nanotubes are positioned on a metal substrate. Having processed the entire body of experimental data, we hypothesized that SWCNT hydrogenation is driven primarily by hydrogen ions.

The comparison of obtained data with parameters $I(D)/I(G)$ reported in [9] for graphene suggests that the efficiency of hydrogenation of nanotubes is lower. Presumably, this is attributable to the fact that hydrogen atoms form bonds primarily with the upper (the most accessible) nanotube layer, while the processes of hydrogen intercalation on the inside are slow. Since a Raman spectrum is an integral characteristic related to the depth of penetration of an incident wave, the data in such a spectrum are „averaged“ over a hydrogenated upper layer and a non-hydrogenated inner layer; therefore, the $I(D)/I(G)$ hydrogenation factor is likely to be higher.

Funding

This study was supported by the Russian Science Foundation, grant No. 21-72-00076.

Conflict of interest

The authors declare that they have no conflict of interest.

References

[1] Q. Peng, J. Crean, L. Han, S. Liu, X. Wen, S. De, A. Dearden. Nanotechnology, Science and Applications, **1** (2014). DOI: 10.2147/NSA.S40324
[2] K.S. Novoselov, A.K. Geim, S.V. Morozov, D. Jiang, Y. Zhang, S.V. Dubonos, I.V. Grigorieva, A.A. Firsov. Science, **306** (5696), 666 (2004). DOI:10.1126/science.1102896
[3] V. Georgakilas, M. Otyepka, A.B. Bourlinos, V. Chandra, N. Kim, K.C. Kemp, P. Hobza, R. Zboril, K.S. Kim. Chem. Rev., **112** (11), 6156 (2012). DOI:10.1021/cr3000412
[4] S.M. Tan, Z. Sofer, M. Pumera. Electroanalysis, **25** (3), 703 (2013). DOI: 10.1002/elan.201200634
[5] D.C. Elias, R.R. Nair, T.M.G. Mohiuddin, S.V. Morozov, P. Blake, M.P. Halsall A.C. Ferrari, D.W. Boukhvalov, M.I. Katsnelson, A.K. Geim, K.S. Novoselov. Science, **323** (5914), 610 (2009). DOI: 10.1126/science.1167130
[6] K.E. Whitener. J. Vacuum Sci. Technol. A, **36** (5), 05G401 (2018). DOI: 10.1116/1.5034433
[7] T. Hussain, A. de Sarkar, R. Ahuja. Appl. Phys. Lett., **101** (10), 103907 (2012). DOI: 10.1063/1.4751249
[8] E.I. Preobrazhensky, I.V. Oladyshkin, M.D. Tokman. Phys. Scripta, **97** (11), 115803 (2022). DOI: 10.1088/1402-4896/ac9564
[9] A. Vodopyanov, E. Preobrazhensky, A. Nezhdanov, M. Zorina, A. Mashin, R. Yakimova, D. Gogova. Superlattices and Microstructures, **160**, 107066 (2021). DOI: 10.1016/j.spmi.2021.107066
[10] M. Wojtaszek, N. Tombros, A. Caretta, P.H.M. van Loosdrecht, B.J. van Wees. J. Appl. Phys., **110** (6), 063715 (2011). DOI: 10.1063/1.3638696
[11] R. Yakimova, C. Virojanadara, D. Gogova, M. Syväjärvi, D. Siche, K. Larsson, L.I. Johansson. Mater. Sci. Forum, **645–648**, 565 (2010). DOI: 10.4028/www.scientific.net/MSF.645-648.565
[12] M. Brzhezinskaya, E.A. Belenkov, V.A. Greshnyakov, G.E. Yalovega, I.O. Bashkin. J. Alloys Compounds, **792**, 713 (2019). DOI: 10.1016/j.jallcom.2019.04.107
[13] M. Brzhezinskaya, V. Shmatko, G. Yalovega, A. Krestinin, I. Bashkin, E. Bogoslavskaja. J. Electron Spectroscopy and Related Phenomena, **196**, 99–103 (2014). DOI: 10.1016/j.elspec.2013.12.013
[14] B.N. Khare, M. Meyyappan, A.M. Cassell, C.V. Nguyen, J. Han. Nano Lett., **2** (1), 73 (2002). DOI: 10.1021/nl015646j
[15] M. Brzhezinskaya, O. Kononenko, V. Matveev, A. Zotov, I.I. Khodos, V. Levashov, V. Volkov, S.I. Bozhko, S.V. Chekmazov, D. Roshchupkin. ACS Nano, **15** (7), 12358 (2021). DOI: 10.1021/acsnano.1c04286
[16] I. Shtepliuk, I.G. Ivanov, T. Iakimov, R. Yakimova, A. Kakanakova-Georgieva, P. Fiorenza, F. Giannazzo. Mater. Sci. Semicond. Processing, **96**, 145 (2019). DOI: 10.1016/j.mssp.2019.02.039
[17] A.C. Ferrari. Solid State Communic., **143** (1–2), 47 (2007). DOI:10.1016/j.ssc.2007.03.052
[18] K.P. Meletov, A.A. Maksimov, I.I. Tartakovskii, J. Arvanitidis, D. Christofilos, G.A. Kourouklis. J. Experimental Theoretical Phys., **112** (6), 979 (2011). DOI: 10.1134/S1063776111040091
[19] A.V. Talyzin, S. Luzan, I.V. Anoshkin, A.G. Nasibulin, H. Jiang, E.I. Kauppinen, V.M. Mikoushkin, V.V. Shnitov, D.E. Marchenko, D. Noréus. ACS Nano, **5** (6), 5132 (2011). DOI: 10.1021/nn201224k
[20] M.S. Dresselhaus, G. Dresselhaus, R. Saito, A. Jorio. Phys. Reports, **409** (2), 47 (2005). DOI: 10.1016/j.physrep.2004.10.006
[21] S.V. Rotkin, S. Subramoney. *Applied Physics of Carbon Nanotubes* (Springer, Berlin, Heidelberg, 2005), DOI: 10.1007/3-540-28075-8

Translated by D.Safin